REVISTA MATÉRIA V.28 N.2
ISSN 1517-7076 articles e20230044, 2023

Development of silver film coating on dental ti15mo alloy to enhance two-body wear resistance, biocompatibility and cytotoxicity effect

Emrah Meletlioğlu[1], Recep Sadeler[1], Sedanur Keleş[1]

[1]Ataturk University, Faculty of Engineering, Department of Mechanical Engineering, 25242, Erzurum, Turkey.
e-mail: emrahmeletli@atauni.edu.tr; receps@atauni.edu.tr; sedanurkelesnano@hotmail.com

ABSTRACT

The basic aim of this in vitro study was to investigate the effects of different silver deposition times on the two-body wear, antibacterial and cytotoxicity properties of silver ions on Ti15Mo alloy. The direct current (DC) magnetron sputtering technique was used to create silver films at different times (30, 45 and 60 minutes); the experimental setup was predetermined. The phase structures, cross-sectional morphology, surface roughness, two-body wear behavior, antibacterial and cytotoxicity properties of all specimens were researched in detail. The surfaces of all films showed a homogeneous distribution. It was observed that silver films enhanced the two-body wear resistance of Ti15Mo alloys. Furthermore, significant correlations were discovered between hardness, surface roughness and wear volume loss. Compared to Ti15Mo alloys, the antibacterial and cytotoxicity test results showed that silver films deposited 30 and 45 min had superior antibacterial and biocompatibility properties.

Keywords: Ti15Mo; DC magnetron sputtering; Two-Body Wear; Antibacterial property; Biocompatibility.

1. INTRODUCTION

Dental biomaterials together with unique mechanical properties, corrosion and fatigue strength, good fatigue resistance and biocompatibility are needed in medical industry [1]. In the area of medical industry, pure titanium (CP-Ti) alloys are used for implant applications because of their low elasticity modulus, excellent strength to weight ratio, superior resistance to corrosion, and easy fabrication, etc. [2, 3]. However, the major disadvantage of the pure titanium (CP-Ti) is that difficulty in polishing, its low strength and poor wear resistance. In view of this, Ti15Mo alloy has attracted interest owing to mechanical and biocompatibility properties [4]. Some studies reported that the Ti15Mo alloy provided good results from better corrosion resistance and higher strength [5]. However, it is still a known that wear is an inevitable problem for implants when used as a metallic antagonist material in dental application. Especially, its unavoidable for the implants placed in the mouth to be exposed to both two-body wear owing to the chewing movement [6]. In addition to this worse condition bacterial infections connected to implants cause inflammation on the surface of the implant, and finally material loss occurs [7].

Despite these drawbacks, many studies are ongoing in an effort to improve coating conditions for healthy use with titanium alloys (for implants and prostheses) [8, 9].

The surface of titanium alloys is coated with antibacterial materials (such as Ag, Cu, ZnKand others) to reduce implant infections, prevent bacterial adhesion, and improve cell viability [10, 11]. Due to its variety of antibacterial features decreased risk of bacterial cells developing resistance, silver stands out among these materials. It is assumed that silver prevents bacterial attachment during and after surgery due to its low toxicity in the human body [12]. Silver particles also interfere with bacterial and other microorganism DNA by penetrating through their cell membranes and walls [13, 14]. As a result, in the case of biomaterials, this type of silver surface functionalization can prevent bacterial colonization, particularly via contact-killing activity. Recently, silver deposition in a nanostructured film demonstrated excellent antibacterial capability as well as increased cell viability during wound healing [15]. Surface modification is a simple and cost-effective method for directly applying antibacterial coatings. Some surface treatment and coating techniques are commonly used to improve the corrosion resistance, mechanical properties, and wear resistance of biomaterials [16]. In particular, DC magnetron sputtering offers advantages over other surface treatments, such as shorter deposition time intervals, the feasibility of uniform surfaces for titanium alloys, and the ability to operate at relatively low temperatures. Optimization of the deposition process is important to achieve the desired

Corresponding Author: Emrah Meletlioğlu Received on 10/02/2023 Accepted on 08/03/2023

DOI: https://doi.org/10.1590/1517-7076-RMAT-2023-0044

properties (wear resistance, biocompatibility, cytotoxicity) in the silver film by sputtering. The effects of deposition parameters such as target angle, argon pressure, substrate bias and temperature on various properties of titanium alloys have been reported in the literature [17, 18]. However, various physical properties (microstructure, surface roughness, hardness, etc.) of these sputter-deposited silver films depend on the deposition parameters and sputtering technique and should be considered for proper film quality control. In protective applications such as biomedical coatings, film thickness has a significant impact on substrate adhesion, structure, and surface properties. Therefore, optimizing the thickness/roughness of the sputtered silver film for coating properties and increasing the efficiency of these processes by determining the factors affecting two-body wear, antimicrobial and cytotoxicity properties are important question in biomedicine.

The basic aim of this in vitro research was to examine the effects of deposition time on the two-body wear, antibacterial and cytotoxicity features of +Ag ions on Ti15Mo.

2. MATERIALS AND METHODS

Ti15Mo alloys with 13 mm thickness were cut from a cylindrical bar with a diameter of 20 mm by Electron Discharge Machine (EDM) and their compositions were obtained from their commercial grades and described elsewhere [19]. The SiC grit papers of different sizes starting from 200 to 1600 were utilized for mechanical polishing of specimens. Afterward, acid etching with an acid solution by mixing 60% H2SO4, 10% HCI and distilled water at a ratio of 1:1:2, respectively, was performed in the fume hood due to increasing adhesion resistance between coating and substrate materials. The etched specimens were cleaned with an ultrasonic bath using deionised water for 10 min. The specimens were dried in air and then placed into the PVD coating system (DC magnetron sputter DAYTAM (Center of East Anatolian High-Technology Research and Application)). The silver target of 3.18 x 50 mm diameter with 99.99% purity was utilized for deposition. We used high-purity (99.999%) argon as the sputtering gas. Process parameters were the angle (target to substrate ~ 35°), distance (target to substrate 11.8 cm), base pressure ($6{,}8 \times 10^{-3}$ mTorr), substrate temperature 50°C, substrate rotation 3 rpm, working gases (argon), and power (DC) 100 W. The actual deposition times for the films were 30 min, 45 min and 60 min, respectively. Depending on the coating times, film thicknesses were also measured. Subsequently, the films were cooled to room temperature in a vacuum. Three specimens were prepared for each condition.

2.1. Microstructural analysis

After the surface treatments, the specimen surface roughness was measured by utilizing a Kla Tencor Stylus Profile instrument. The phase structure of both untreated and silver-coated specimens was investigated by X-ray diffraction (Explorer, GNR, Italy) using Cu Kα radiation (λ = 1.5418 Å) and JCPDS PDF-2 database. Scanning electron microscope (FEI Quanta FEG 250, USA) examinations were conducted to observe surface and cross-section morphologies image of the coated and tested specimens. Hardness measurements were carried out by a micro-hardness tester (Wolpert Wilson Instruments) under indentation load of 25 g and loading time of 10 s. Seven different area were chosen randomly and the result was an average value with standard deviation.

2.2. Two-body wear tests

Computer-controlled chewing simulator was designed and manufactured to evaluate two-body wear of Ti15Mo illustrated in Figure 1. Two-body wear tests were performed to 50 N mechanical force, 240.000 wear cycles (an average of two years in vivo experiment), 2.0 Hz wear frequency, 37°C ± 1°C under atmospheric conditions,

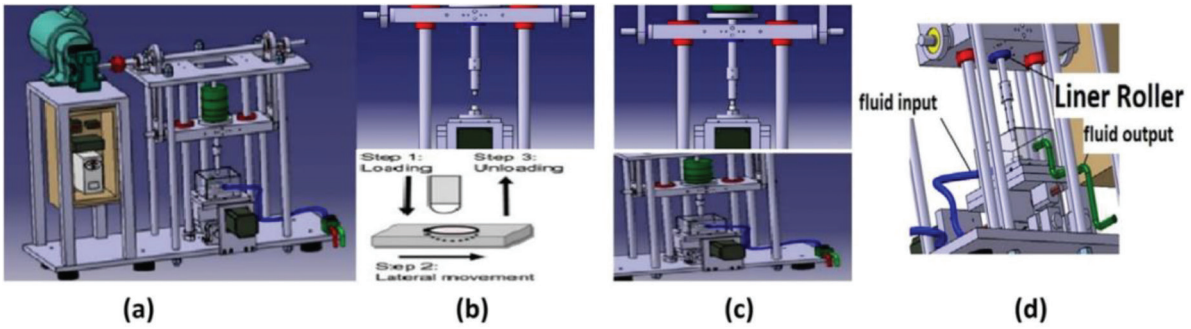

Figure 1: Schematics of the computer-controlled chewing simulator test device: (a) general view of the device; (b) mechanical loading unit; (c) without lateral movement loading; (d) thermal unit.

Table 1: Chemical composition of the Butt's solution [20].

REAGENT	COMPOSITION (G/L)
NaCl	0.4 g
KCl	0.4 g
$CaCl_2.2H_2O$	0.9 g
$(CO(NH_2)_2)$	1 g
$NaH_2PO_4.2H_2O$	0.7 ml
$Na_2S.9H_2O$	0.005 g

6 mm diameter steatite ball Al_2O_3, 0.7 mm lateral movement in pH artificial saliva (pH:7) respectively. A modified Butt's artificial saliva (Table 1) was formulated in order to tribocorrosion tests [20]. The bite force occurring in the chewing cycle (50 N) was kept stable along the experiment using dead weight (5 kg).

At the end of the two-body wear tests, 2D and 3D profilometer images were taken and analyzed for volume loss on the wear surfaces (using noncontact profilometer Bruker-Contour GT 3D). The data obtained were analyzed using statistical software (SPSS Statics 20.0 for Windows 64 bit; SPSS Inc., Chicago, IL, USA). The means and standard deviations of Ra, HV, and volume loss were calculated and analyzed using the one-way ANOVA. The Games Howell test was used for a post hoc analysis. The significance level was set to $\alpha = 0.00001$.

2.3. Antibacterial activity

The plate counting process (accordance with National Standart of China GB/T 4789.2 protocol) was utilized to quantify the antibacterial features of Ti15Mo alloys [19, 20]. Two bacterial species, *Escherichia coli* ATCC25922 and *Staphylococcus aureus* ATCC25923 were selected for testing. Frozen powders of the bacteria were dissolved in a culture medium with pH ¼ 7.2, cultivated at 37 °C for 24 h. Afterwards a bacterial suspension was obtained. Then 100 μL volume of an inoculated bacterial solution with proximate concentration of ~4×10^8 colony forming unit per millilitre (CFU/mL) was used on each sample. After a 24-hour incubation time at 37°C, the number of colonies created by the growth of viable bacteria on the sample was counted. The colony forming unit (CFU) per millilitre of culture solution was calculated with the formula:

$$\text{CFU/mL} = (\text{Number of colonies/Capacity of culture in the plate}) \times \text{Dilution factor.}$$

Dilution factor was defined as the ratio of final volume of bacterial suspension after dilution to the volume of bacterial suspension before dilution.

2.4. Cytotoxicity assay

L929 Cell Line (American Type Culture Collection, USA) were incubated in Dulbecco's modified Eagle's medium (DMEM) supplemented with a 10% fetal bovine serum (FBS), at 37°C in a humidified atmosphere of 5% CO_2. Cells were counted after successive passage and seeded at 1×10^6 cells/mL in each well in the 6-well plate. The cells were incubated in a CO_2 extrude for 24 hours to settle at the bottom of the well. After 24 h of incubation at 37°C in a humidified atmosphere of 5% CO_2, cells were incubated with MTT solution ((3-(4,5-dimethylthiazole-2-yl)-2,5-diphenyl tetrazolium bromide; Sigma Aldrich) for 2 h at 37°C. Spectrophotometric reading at 570 nm was performed, using a microplate reader (Epoch Microplate Spectrophotometer, USA) and results were expressed as percentage of cell viability. The cell images in fields were taken under a fluorescence microscope (Leica DMIL LED). Each experiment was carried out 4 times (n = 4).

3. RESULTS AND DISCUSSION

3.1. Microstructures

Figure 2 shows the variation in the XRD patterns of Ti15Mo alloys. The untreated Ti15Mo alloys are illustrated in Figure 2(a), where the diffractograms have peaks typical of a single crystalline structure (110, 200), which is typical of the alloys phase (96-900-8555) [21, 22]. The XRD patterns of the silver films deposited at various deposition times of 30, 45, and 60 min are displayed in Figure 2(b). According to the XRD results, the silver phases (96-500-0219) were generated with a preferred orientation in the direction (111), with minor contributions in the directions (200), (202), and parallel plane (311). Because silver has a cubic structure, it is possible that the majority of nanoparticle-like structures are formed by crystallites with cubic faces parallel to the substrate (single crystalline) [23]. When the film is more than 1.6 μm thick (60 min coated), the structure of sputter-deposited

silver films exhibited a preferred orientation in the (111) direction. The cubic phases (face-centered cubic), were parallel to the substrate surface.This preferred orientation in the (111) direction was also noticed for silver films deposited by sputtering [24]. XRD indicates that this is indeed the case. When the film thickness increases, there is a coalescence of these crystallites, but they do not interact in the same crystal planes. According to the Scherrer equation, this crashing coalescence contributes to large grains with crystallites growing in all directions, especially (111) as expected for a crystalline solid [25].

Figure 3 displays the cross-sectional SEM micrographs of all films. According to results, thin film thickness values were increased with the increase in coating times (Figure 3a–3c). The increments in the coating time gave rise to merged nano-columnar growth. This may be attributed to the surface-diffusion influence where

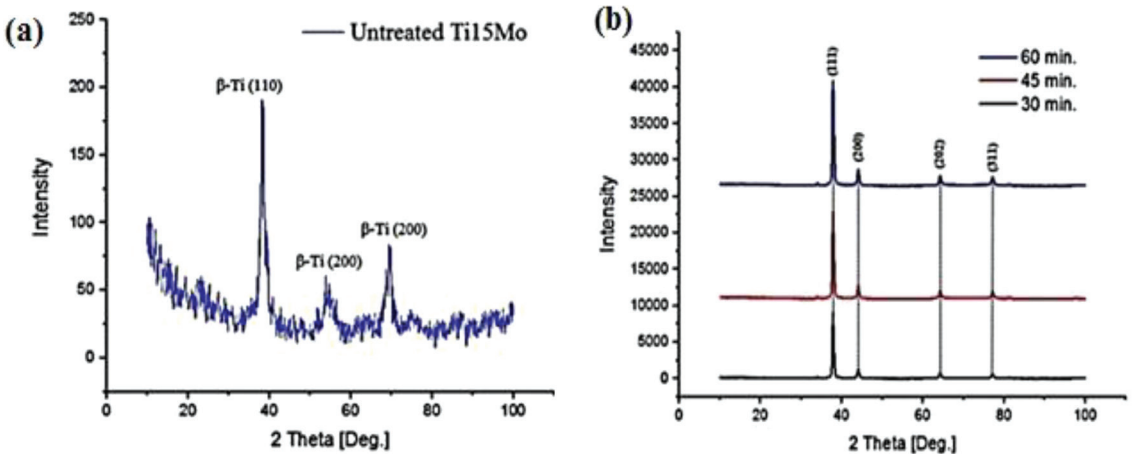

Figure 2: XRD results: (a) untreated Ti15Mo; (b) Silver-coated Ti15Mo.

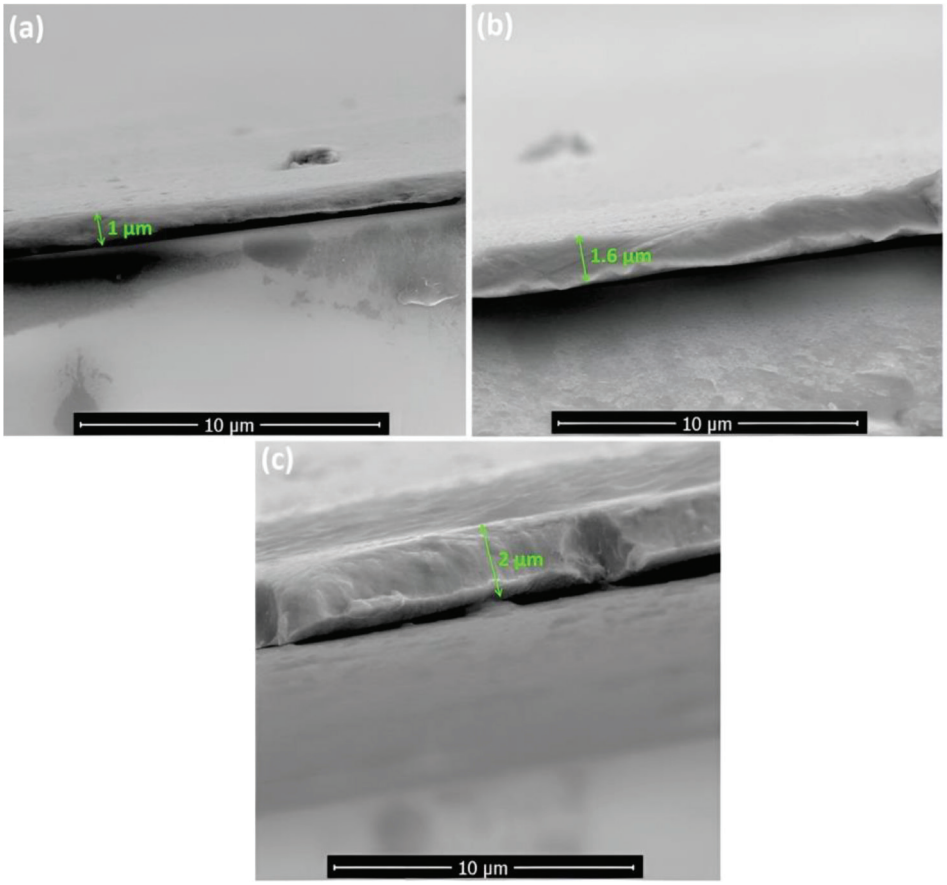

Figure 3: Cross-section SEM micrographs observed for silver-coated alloys: (a) 30 min; (b) 45 min; (c) 60 min.

a longer coating time (45–60 min) finally caused an increase in the temperature (20 to 37°C) that increased the adatom mobility (Figure 3b–3c). Also, the nano-columnar growth of the silver films tends to bend with increasing film thickness [26].

The average surface hardness of untreated specimens is HV = 230. A decrease of coatings hardness was observed with silver ion additions, owing to the incorporation of the soft silver on the structure. Surface roughness of untreated specimens was Ra = 0.152 – 0.241 μm. The average surface roughness values of the alloys decreased after the mechanical polishing process (Ra = 0.085–0.096 μm). Surface roughness values increased after the acid-etching process (Ra = 2.110–2.126 μm). After the coating process, all specimens had low surface roughness. Moreover, the lowest surface roughness was observed for the 30-minute coating time among all coatings because of finer grain sizes.

3.2. Two-body wear tests

Table 2 shows the hardness, roughness and mean volume loss values of the specimens tested in this study. Throughout the test, 30 min silver-coated Ti15Mo alloy showed less wear volume loss than other coated specimens as shown in Table 2. In fact, it has been reported to exhibit better wear strength with added +Ag elements to titanium alloys [27]. However, the measured wear volume loss presented at the end of the test in artificial saliva is found to be obvious increase along with the increasing of silver content. It was seen that while Ag coated increasing to 60 min, accompanied by decreasing of hardness, leading to a continuous degradation of the wear strength owing to the concomitant softening of the coating [28].

Table 3 shows the one-way ANOVA results for the hardness, surface roughness and wear volume loss. In this study, correlations between the hardness, surface roughness and wear volume loss were found to be significant. A study in the literature reported that Ti alloys specimen presented lower wear volume loss that may be linked to its higher hardness values compared to the other alloys [29]. 2-dimensional non-contact profilometer volume loss analysis of the Ti15Mo alloys after the two-body wear tests in the artificial saliva environment are given in Figure 4. The highest wear depth was observed in 60 min coated Ti15Mo while the lowest wear depth was observed in untreated Ti15Mo alloys.

Figure 5 displays an instance of the 3-dimensional non-contact profilometer test specimen and wear area analyses of the Ti15Mo alloys after the two-body wear tests. The surface of the coated Ti15Mo alloys in the non-wear is very low, as shown in Figure 5(b). This result shows that there is no hydraulic degradation in coated Ti15Mo alloys artificial saliva through chewing test procedures. When considering coating times, it is clear that limiting the optimization of the coating time of Ti15Mo alloys, which has a new field of application in the field of dentistry, is critical in terms of wear resistance.

3.3. Antibacterial properties

The plate counting process was used to evaluate the antibacterial effect of untreated and silver-coated titanium specimens. The optical photographs showing a range of viable bacteria found in each specimen are presented in

Table 2: Hardness, surface roughness and mean volume loss values of the Ti15Mo alloys tested in this study (standard deviation).

	UNTREATED	30 min	45 min	60 min
Surface Roughness (μm)	0.220 (0.02)	0.210 (0.01)	0.240 (0.01)	0.280 (0)
Hardness (HV)	230 (94.87)	132 (39.53)	115 (18.97)	101 (14.23)
Volume Loss (mm^3 x 10^{-1})	0.23 (0.11)	0.28 (0.18)	0.485 (0.18)	0.63 (0.19)

Table 3: Data of One-Way ANOVA Analyses for the Mean Wear Volume Loss of Ti15MO alloys. (Regression analysis the relation between surface roughness, Hardness and the mean wear volume loss.) (df: degree of freedom, F ratio: analysis of variance).

FACTORS	SUM OF SQUARES	df	MEAN SQUARE	F RATIO	SIGNIFICANCE
Surface Roughness (μm)	0.065	7	.009	96.642	<0.00001
Hardness (HV)	213450.800	7	32635.829	22.501	<0.00001
Volume Loss (mm^3 x 10^{-1})	8.704	7	.903	149.261	<0.00001

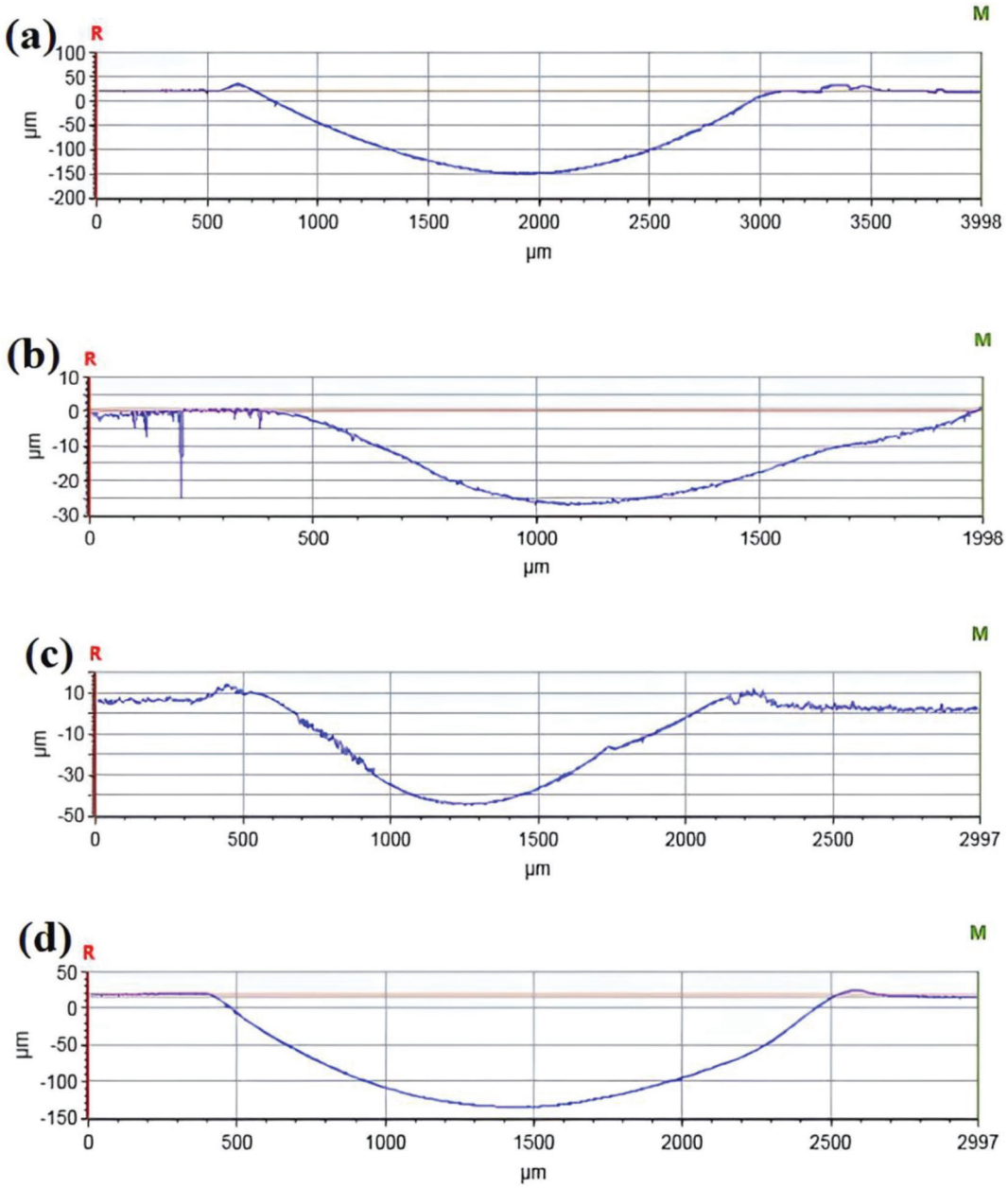

Figure 4: Two-dimensional non-contact profilometer volume loss analysis of the Ti15Mo alloys after the two-body wear tests in the artificial saliva (pH:7) environment. (a) Untreated (b) 30 min; (c) 45 min; (d) 60 min.

Figure 6. A colony is formed from a single living bacterium. Bacterial film formation was observed in untreated titanium alloys. This means that there is a large number of visible bacteria on the untreated titanium surface. On the other hand, the silver-coated titanium surfaces were prone to decreases in the growth of *E. coli* and *S. aureus* bacteria. According to the results, the colonies of bacteria gradually decreased with the increase in silver deposition time (Figure 6(b–d)). It can said that, degradation of magnetron sputter technique silver coating (1 µm) layer may also take place allowing silver ion leaching into the bacterial solution during incubation as observed with thin silver layers. But, more uniform and conformal coating was obtained with increasing layer thickness and as a result, thicker films exhibited better antibacterial properties as bacteria could not reach the titanium surface. The CFU/mL value was calculated for each specimen and then illustrated in Figure 7 On untreated titanium specimen surfaces, the numbers of bacterial colonies were substantially high compared to silver-coated titanium specimens. According to Figure 7, the ability of silver-coated Ti15Mo surface to suppress the growth of *E. coli* was less effective than *S. aureus*. This situation is thought to be associated with the spherical form of *S. aureus*, which provides a wide surface field for the Ag+ ion to react [30]. There are two main reasons behind the good antibacterial property of the silver-coated Ti15Mo surface. The first reason is the role of the Ag+ ion

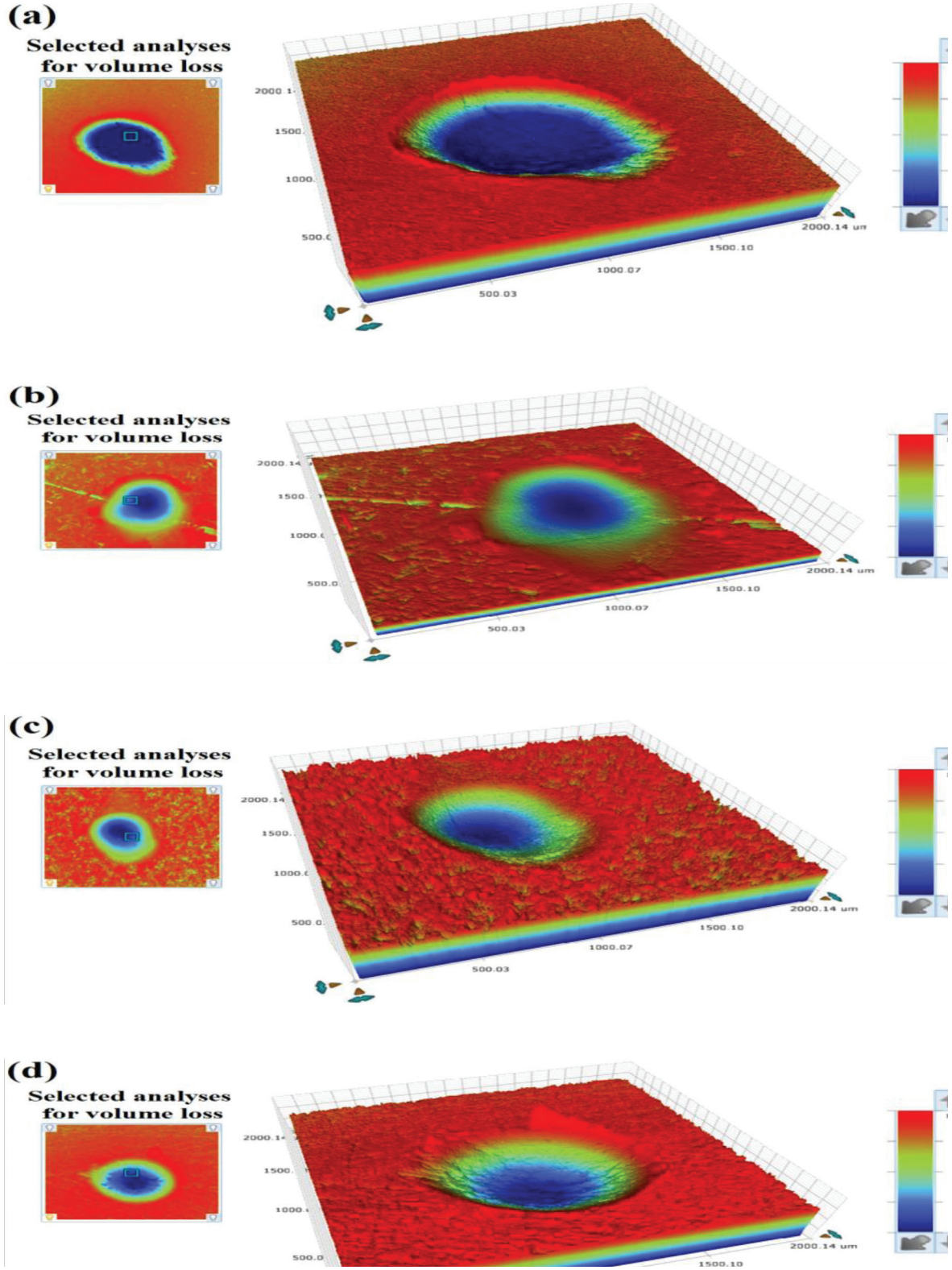

Figure 5: 3-dimensional non-contact profilometer wear area analyses of the Ti15Mo alloys after the two-body wear tests in the artificial saliva (pH:7) environment (a) untreated (b) 30 min; (c) 45 min; (d) 60 min.

which comes in contact with the outer cell wall and causes oxidative stress with the help of reactive oxygen species and then destroys the cell membrane [31]. Once membranes break down, the silver ion enters the cytoplasm and eliminates the intracellular structures. The other reason is the direct physical contact among bacterial cells and specimen nanoparticles present on the silver-coated Ti15Mo alloy surface. This may be attributed to the direct contact surface causing the cell wall of the bacteria to become strained and damaged.

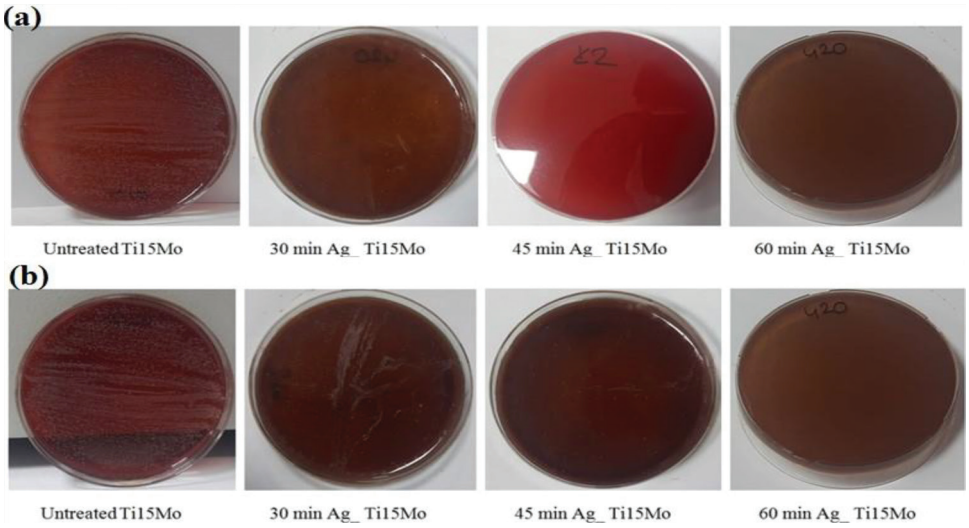

Figure 6: Surface colonization results for: (a) E. coli; (b) S. aureus; after 24 hours.

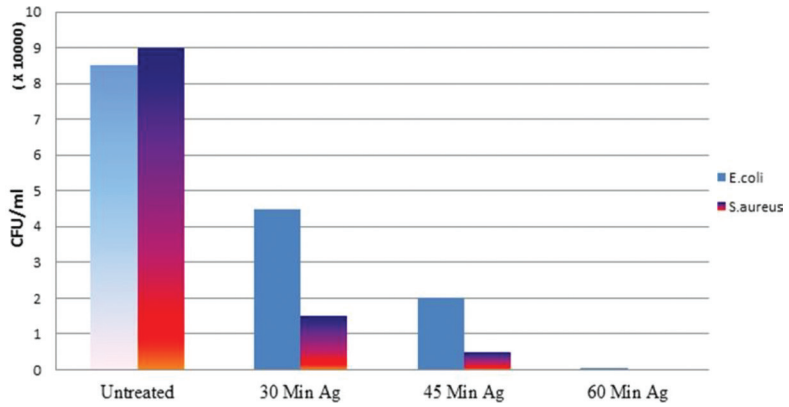

Figure 7: The CFU/mL value of Ti15Mo surface against *S. aureus* and *E. coli*.

The analysis of these results allows concluding that the magnetron sputter technique silver-coated alloys yields a reduction in the bacterial growth. The bactericide effect of the specimen with 60 min coated resulted especially interesting, in which no bacteria colony was found at the dilution. As the antibacterial test conditions were same for all the specimens, the differences in antimicrobial effect can be directly attributed to the Ag+ release time into the environment. The ion release of Ag+ is influenced by the parameters of sputter coated but also affected by other parameters as film microstructure, particle size and distribution in the film thickness and target angle, which can limit the access of electrolyte and particle dissolution. Particularly, the segregation of silver in the surface forming aggregates over the time is of extreme importance in order to estimate quantitatively the antibacterial effect and additional experiments are advisable. Nevertheless, a positive response of silver doping for prevention of infection with *E. coli* and *S.aureus* were proved in all cases but considering that coated above 45 min have demonstrated cytotoxic effects [32], the silver doping should be restricted below this threshold.

3.4. Cytotoxicity assessment

Excessive presence of silver can be toxic to the human body [32, 33], so it was very important to perform cytotoxicity testing to determine the magnetron sputter coating time. The cytotoxic evaluation was performed by accepting the cell viability of the healthy as 100%. Figure 8 presents the effect of silver coatings on the L929 cell viability (after 24 h) examined using MTT assay. If cell viability exceeds 70% in the presence of any specimen, it is called a nonstotoxic material according to accepted standard (ISO 10993–5). Both the 30 min and the 45 min silver-coated alloys exhibited non-toxic properties because of the cell viability was significantly higher than 70% indicating the determineted process did not cause any toxicity in the coated Ti15Mo alloys according to ISO 10993–5 standard. It is known that silver ions are nonstoxic and increase cell viability [34]. However, the

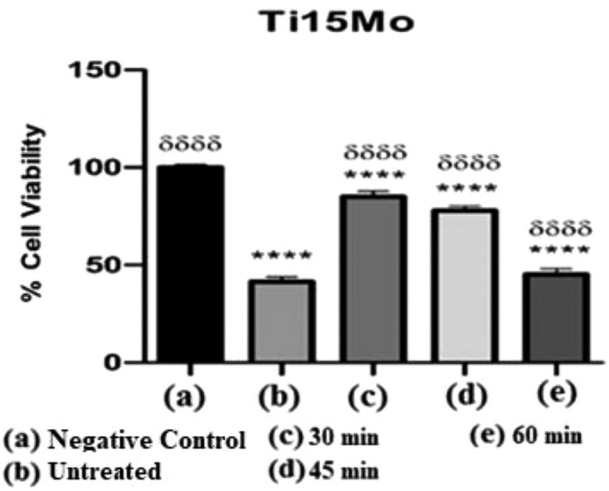

Figure 8: Cytotoxicity test with L929 cell viability (a) Negative Control; (b) Untreated (c) 30 min; (d) 45 min; (e) 60 min.

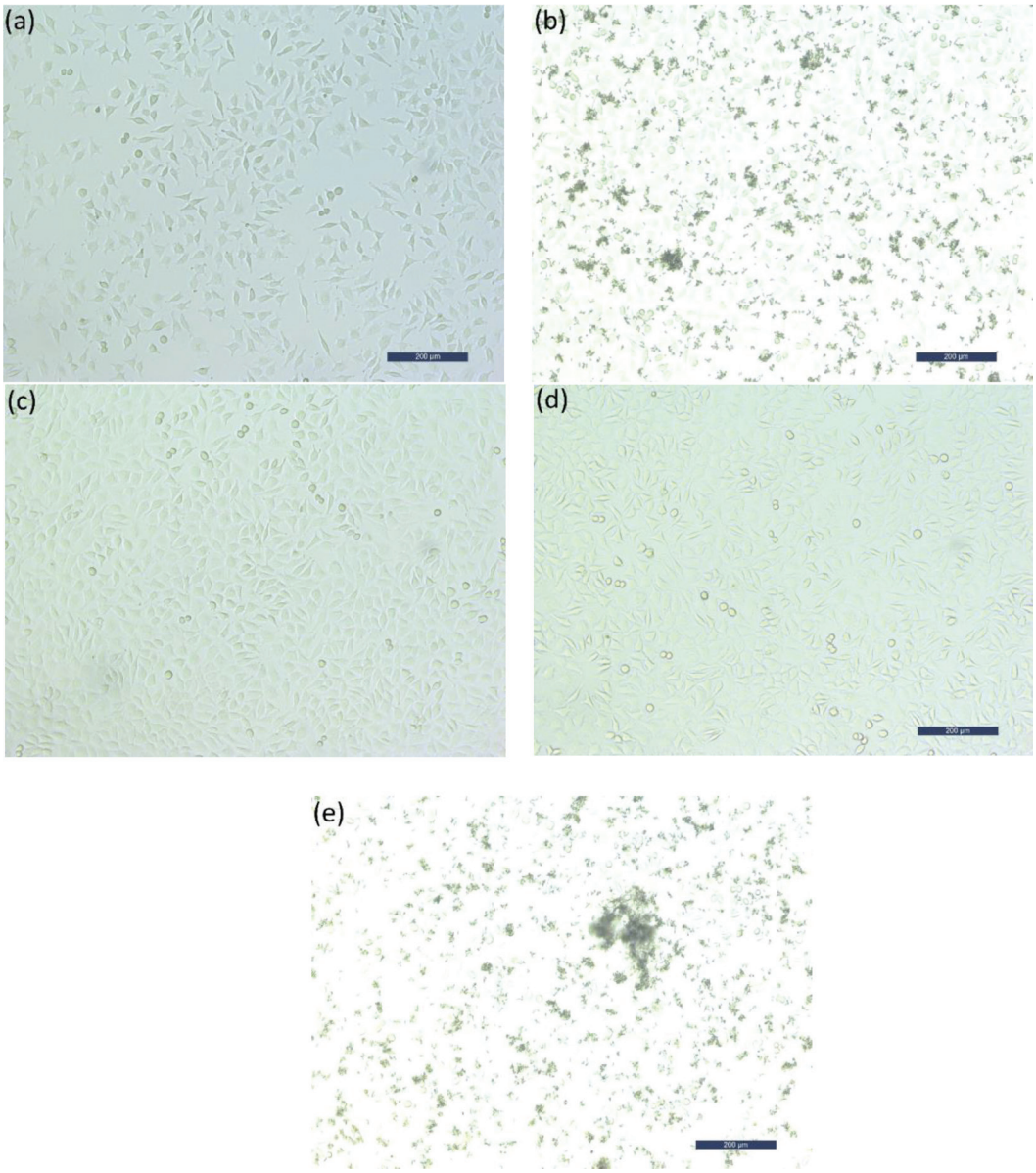

Figure 9: Optical microscope images of L929 fibroblast cell morphologies of Ti15Mo alloys (a) Negative Control; (b) Untreated (c) 30 min; (d) 45 min; (e) 60 min.

cell viability percentage of 60 min coated Ti15Mo alloys were lower than the others. In our study, the difference in cell viability between coated specimens may originate from the release of +Ag ions that can affect cell viability. It is well known that Although +Ag ions are useful in terms of its antimicrobial property, it can exhibit a toxic behavior at high concentrations [35]. It can be said that the film thickness values of (1–1.60 um) used in the coated of silver was appropriate for toxicity.

The respective optical microscopic morphologies of L929 cell line after 24 h of culture are displayed in Figure 9. Also, on the 30 min and 45 min coated substrates, we could see that the cells extended with their filopodia and attempted to pick up the largest possible area on the coating, regardless of the substrate type. These data clearly demonstrate the high biocompatibility of both types of tested coated (compare micrographs in Figure 9c–d), supporting the results from the MTT assay. However, it can be seen in Figure 9e that the cells on substrates coated for 60 min did not elongate with their filopodia and could not be effective on the coating regardless of the substrate type.

4. CONCLUSIONS

Our study showed that while β-Ti phase peaks were seen on uncoated alloy surfaces, Ag peaks were observed with diffraction from the coated alloys after the coating process. All alloys had low surface roughness compared to acid-etched uncoated alloys and the lowest surface roughness value was obtained for alloys with silver deposited for 30 min. The thin film thickness values increased with increasing treatment time. Within the limitations of the present study, the hardness of the Ti15Mo alloy was significantly greater than the coated alloys.

Throughout the two-body wear test, 30 min silver-coated Ti15Mo alloy showed less wear volume loss than other coated specimens. This can be explained by the surface hardness value of the alloy. In this study, correlations between the hardness, surface roughness and wear volume loss were found to be significant.

The magnetron sputter coating process enhanced the antibacterial activity of Ti15Mo alloys owing mainly to the formation of the silver film on the substrate. The Ti15Mo alloys had strong long-term antibacterial activity (≥99%) even after being immersed in bacterial solution for up to 24 hours. The ionic release of Ag+ is influenced by the parameters of sputter coating, but also is affected by other parameters like film microstructure, particle size and distribution in the film thickness and target angle, which can limit the access of electrolyte and particle dissolution. Particularly, the segregation of silver in the surface forming aggregates over the time has extreme importance in order to quantitatively estimate the antibacterial effect and additional experiments with statistical analysis are advisable.

Both the 30 min and the 45 min silver-coated alloys exhibited non-toxic properties because of the cell viability was significantly higher than 70% indicating the determined process did not cause any toxicity in the coated Ti15Mo alloys according to ISO 10993–5 standards. However, the cell viability percentage of 60 min coated Ti15Mo alloys were lower than the others. In our study, the difference in cell viability between coated specimens may originate from the release of +Ag ions that can affect cell viability. It can be said that the film thickness values of (1–1.60 um) used in the coated of silver was appropriate for toxicity.

5. ACKNOWLEDGMENTS

This work was supported by Ataturk University the Coordination Unit of Scientific Research Projects [grant number PRJ7393] The authors thanks the Ataturk University Faculty of Medicine Department of Medical Pharmacology and Medical Microbiology for providing laboratory facilities and access to equipment.

6. REFERENCES

[1] LIU, H., YANG, J., ZHAO, X., *et al*., "Microstructure, mechanical properties and corrosion behaviors of biomedical TiZr-Mo-xMn alloys for dental application", *Corrosion Science*, v. 161, pp. 2–15, 2019. doi: http://dx.doi.org/10.1016/j.corsci.2019.108195.

[2] MARIANO, N., OLIVEIRA, R.G., FERNANDES, M.A., *et al*., "Corrosion behavior of pure titanium in artificial saliva solution", *Matéria (Rio de Janeiro)*, v. 14, n. 2, pp. 878–880, 2009. doi: http://dx.doi.org/10.1590/S1517-70762009000200010.

[3] PEÓN AVÉS, E., SADER, M.S., JERÔNIMO, F.A.R., *et al*., "Comparative study of hydroxyapatite coatings obtained by Sol-Gel and electrophoresis on titanium sheets", *Matéria (Rio de Janeiro)*, v. 12, n. 1, pp. 156–163, 2007. doi: http://dx.doi.org/10.1590/S1517-70762007000100020.

[4] MARTINS JÚNIOR, J.R.S., NOGUEIRA, R.A., ARAÚJO, R.O., *et al*., "Preparation and characterization of Ti-15Mo alloy used as biomaterial", *Materials Research*, v. 14, n. 1, pp. 107–112, 2011. doi: http://dx.doi.org/10.1590/S1516-14392011005000013.

[5] HACISALIHOGLU, I., SAMANCIOGLU, A., YILDIZ, F., *et al*., "Tribocorrosion properties of different type titanium alloys in simulated body fluid", *Wear*, v. 332, pp. 679–686, 2015. doi: http://dx.doi.org/10.1016/j.wear.2014.12.017.

[6] MAHAMOOD, R.M., AKINLABI, E.T., "Laser metal deposition of functionally graded Ti6Al4V/TiC", *Materials & Design*, v. 84, pp. 402–410, 2015. doi: http://dx.doi.org/10.1016/j.matdes.2015.06.135.

[7] NAG, S., BANERJEE, R., FRASER, H.L., "Microstructural evolution and strengthening mechanisms in Ti-Nb-Zr-Ta, Ti-Mo-Zr-Fe and Ti-15Mo biocompatible alloys", *Materials Science and Engineering C*, v. 25, n. 3, pp. 357–362, 2005. doi: http://dx.doi.org/10.1016/j.msec.2004.12.013.

[8] NAKAGAWA, M., MATONO, Y., MATSUYA, S., *et al*., "The effect of Pt and Pd alloying additions on the corrosion behavior of titanium in fluoride-containing environments", *Biomaterials*, v. 26, n. 15, pp. 2239–2246, 2005. doi: http://dx.doi.org/10.1016/j.biomaterials.2004.07.022. PubMed PMID: 15585225.

[9] YANOVSKA, A.A., STANISLAVOV, A.S., SUKHODUB, L.B., *et al*., "Silver-doped hydroxyapatite coatings formed on Ti-6Al-4V substrates and their characterization", *Materials Science and Engineering C*, v. 36, pp. 215–220, 2014. doi: http://dx.doi.org/10.1016/j.msec.2013.12.011. PubMed PMID: 24433906.

[10] PEREIRA, B.L., TUMMLER, P., MARINO, C.E.B., *et al*., "Titanium bioactivity surfaces obtained by chemical/electrochemical treatments", *Matéria (Rio de Janeiro)*, v. 19, n. 1, pp. 16–23, 2014. doi: http://dx.doi.org/10.1590/S1517-70762014000100004.

[11] ELIAS, C.N., FERNANDES, D.J., RESENDE, C.R., *et al*., "Mechanical properties, surface morphology and stability of a modified commercially pure high strength titanium alloy for dental implants", *Dental Materials Journal*, v. 31, n. 2, pp. e1–e13, 2015. doi: http://dx.doi.org/10.1016/j.dental.2014.10.002. PubMed PMID: 25458351.

[12] LICHTER, J.A., VAN VLIET, K.J., RUBNER, M.F., "Design of antibacterial surfaces and interfaces: polyelectrolyte multilayers as a multifunctional platform", *Macromolecules*, v. 42, n. 22, pp. 8573–8586, 2009. doi: http://dx.doi.org/10.1021/ma901356s.

[13] BAKHSHESHI-RAD, H.R., ISMAIL, A.F., AZIZ, M., *et al*., "Co-incorporation of graphene oxide/silver nanoparticle into poly-L-lactic acid fibrous: a route toward the development of cytocompatible and antibacterial coating layer on magnesium implants", *Materials Science and Engineering C*, v. 111, pp. 110812, 2020. doi: http://dx.doi.org/10.1016/j.msec.2020.110812. PubMed PMID: 32279830.

[14] ZHANG, Y., LIU, X., LI, Z., *et al*., "Nano Ag/ZnO-incorporated hydroxyapatite composite coatings: highly effective infection prevention and excellent osteointegration", *ACS Applied Materials & Interfaces*, v. 10, n. 1, pp. 1266–1277, 2018. doi: http://dx.doi.org/10.1021/acsami.7b17351. PubMed PMID: 29227620.

[15] STUART, B.W., STAN, G.E., POPA, A.C., *et al*., "New solutions for combatting implant bacterial infection based on silver nano-dispersed and gallium incorporated phosphate bioactive glass sputtered films: a preliminary study", *Bioactive Materials*, v. 8, pp. 325–340, 2021. doi: http://dx.doi.org/10.1016/j.bioactmat.2021.05.055. PubMed PMID: 34541404.

[16] TAGLIETTI, A., ARCIOLA, C.R., D'AGOSTINO, A., *et al*., "Antibiofilm activity of a monolayer of silver nanoparticles anchored to an amino-silanized glass surface", *Biomaterials*, v. 35, n. 6, pp. 1779–1788, 2014. doi: http://dx.doi.org/10.1016/j.biomaterials.2013.11.047. PubMed PMID: 24315574.

[17] FORDHAM, W.R., REDMOND, S., WESTERLAND, A., *et al*., "Silver as a bactericidal coating for biomedical implants", *Surface and Coatings Technology*, v. 253, pp. 52–57, 2014. doi: http://dx.doi.org/10.1016/j.surfcoat.2014.05.013.

[18] DEL RE, M., GOUTTEBARON, R., DAUCHOT, J.P., *et al*., "Growth and morphology of magnetron sputter deposited silver films", *Surface and Coatings Technology*, v. 151, pp. 86–90, 2002. doi: http://dx.doi.org/10.1016/S0257-8972(01)01592-4.

[19] YU, W., LI, X., HE, J., *et al*., "Graphene oxide-silver nanocomposites embedded nanofiber core-spun yarns for durable antibacterial textiles", *Journal of Colloid and Interface Science*, v. 584, pp. 164–173, 2021. doi: http://dx.doi.org/10.1016/j.jcis.2020.09.092. PubMed PMID: 33069016.

[20] HACISALIOGLU, I., *et al*., "Wear behavior of the plasma and thermal oxidized Ti-15Mo and Ti-6Al-4V alloys, in IOP Conference Series", *Materials Science and Engineering*, v. 174, pp. 012055, 2007.

[21] SABEENA, M., GEORGE, A., MURUGESAN, S., *et al*., "Microstructural characterization of transformation products of bcc β in Ti-15 Mo alloy", *Journal of Alloys and Compounds*, v. 658, pp. 301–315, 2016. doi: http://dx.doi.org/10.1016/j.jallcom.2015.10.200.

[22] SZKLARSKA, M., DERCZ, G., RAK, J., *et al*., "The influence of passivation type on corrosion resistance of Ti15Mo alloy in simulated body fluids Arc", *Metals and Materials*, v. 60, n. 4, pp. 2687–2694, 2015. doi: http://dx.doi.org/10.1515/amm-2015-0433.

[23] ANDRADE, J.E.D., MACHADO, R., MACÊDO, M.A., *et al*., "AFM and XRD characterization of silver nanoparticles films deposited on the surface of DGEBA epoxy resin by ion sputtering", *Polímeros*, v. 23, n. 1, pp. 19–23, 2013. doi: http://dx.doi.org/10.1590/S0104-14282013005000009.

[24] MARECHAL, N., QUESNEL, E.A., PAULEAU, Y., "Silver thin films deposited by magnetron sputtering", *Thin Solid Films*, v. 241, n. 1–2, pp. 34–38, 1994. doi: http://dx.doi.org/10.1016/0040-6090(94)90391-3.

[25] ÇOMAKLI, O., YAZICI, M., YETIM, T., *et al*., "The effects of aging time on the structural and electrochemical properties of composite coatings on Cp-Ti substrate", *Journal of Bionics Engineering*, v. 14, n. 3, pp. 532–539, 2017. doi: http://dx.doi.org/10.1016/S1672-6529(16)60419-5.

[26] PHAE-NGAM, W., CHANANONNAWATHORN, C., LERTVANITHPHOL, T., *et al*., "Effect of deposition time on nanocolumnar TiZrN films grown by reactive magnetron co-sputtering with the OAD technique", *Mater Technol (N Y N Y)*, v. 55, n. 1, pp. 65–70, 2021. doi: http://dx.doi.org/10.17222/mit.2019.189.

[27] DONG, M., ZHU, Y., XU, L., *et al*., "Tribocorrosion performance of nano-layered coating in artificial seawater", *Applied Surface Science*, v. 487, pp. 647–654, 2019. doi: http://dx.doi.org/10.1016/j.apsusc.2019.05.119.

[28] KÖSTENBAUER, H., FONTALVO, G.A., MITTERER, C., *et al*., "Tribological properties of TiN/Ag nanocomposite coatings", *Tribology Letters*, v. 30, n. 1, pp. 53–60, 2008. doi: http://dx.doi.org/10.1007/s11249-008-9312-7.

[29] MAO, C., XIANG, Y., LIU, X., *et al*., "Photo-inspired antibacterial activity and wound healing acceleration by hydrogel embedded with Ag/Ag@ AgCl/ZnO nanostructures", *ACS Nano*, v. 11, n. 9, pp. 9010–9021, 2017. doi: http://dx.doi.org/10.1021/acsnano.7b03513. PubMed PMID: 28825807.

[30] ABED, S., BAKHSHESHI-RAD, H.R., YAGHOUBI, H., *et al*., "Antibacterial activities of zeolite/silver-graphene oxide nanocomposite in bone implants", *Materials Technology*, v. 36, n. 11, pp. 660–669, 2021. doi: http://dx.doi.org/10.1080/10667857.2020.1786784.

[31] MIHAILESCU, I.N., BOCIAGA, D., SOCOL, G., *et al*., "Fabrication of antimicrobial silver-doped carbon structures by combinatorial pulsed laser deposition", *International Journal of Pharmaceutics*, v. 515, n. 1–2, pp. 592–606, 2016. doi: http://dx.doi.org/10.1016/j.ijpharm.2016.10.041. PubMed PMID: 27773854.

[32] VAZQUEZ-MUÑOZ, R., BORREGO, B., JUÁREZ-MORENO, K., *et al*., "Toxicity of silver nanoparticles in biological systems: does the complexity of biological systems matter?", *Toxicology Letters*, v. 276, pp. 11–20, 2017. doi: http://dx.doi.org/10.1016/j.toxlet.2017.05.007. PubMed PMID: 28483428.

[33] HADRUP, N., LAM, H.R., "Oral toxicity of silver ions, silver nanoparticles and colloidal silver - a review", *Regulatory Toxicology and Pharmacology*, v. 68, n. 1, pp. 1–7, 2014. doi: http://dx.doi.org/10.1016/j.yrtph.2013.11.002. PubMed PMID: 24231525.

[34] SUNDERMAN JUNIOR, F.W., "Metal carcinogenesis in experimental animals", *Food and Cosmetics Toxicology*, v. 9, n. 1, pp. 105–120, 1971. doi: http://dx.doi.org/10.1016/S0015-6264(71)80120-7. PubMed PMID: 4996513.

[35] ERDEM, U., DOGAN, M., METIN, A.U., *et al*., "Hydroxyapatite-based nanoparticles as a coating material for the dentine surface: an antibacterial and toxicological effect", *Ceramics International*, v. 46, n. 1, pp. 270–280, 2020. doi: http://dx.doi.org/10.1016/j.ceramint.2019.08.260.